SQT

NASA Technical Memorandum 78690

(NASA-TM-78690) A NEW BOUNDARY-LAYER INTERACTION TECHNIQUES FOR SEPARATED FLOWS (NASA) 26 p HC A03/MF AC1 CSCL 01A
N79-16802
Unclas
G3/02 14248

A NEW BOUNDARY-LAYER INTERACTION TECHNIQUE FOR SEPARATED FLOWS

James E. Carter

June 1978

National Aeronautics and
Space Administration

Langley Research Center
Hampton, Virginia 23665

SUMMARY

A new viscous-inviscid interaction procedure is presented which is applicable to separated flows. The new procedure is simple, converges rapidly, and does not require numerical smoothing and underrelaxation, at least in the cases computed thus far. Calculations are presented for the low speed separated flow in the juncture region between an axisymmetric body and sting. The viscous computation is done with an inverse boundary-layer procedure which was previously developed. The inviscid computation is made with an axisymmetric transonic code called RAXBOD. The main advantage of the new interaction procedure is that it combines an inverse boundary-layer technique, which is applicable to separated flows, with an existing inviscid analysis code with only a slight boundary condition change required in the inviscid code.

INTRODUCTION

An accurate prediction of the aerodynamic forces on a vehicle requires that the interaction between the viscous and inviscid flow be taken into account, particularly near the aft end where the thickness of the viscous layer is significant and separation often occurs. If separation is present, conventional matching of the boundary-layer and inviscid flow is divergent since the boundary-layer solution is singular at the separation point, resulting in a displacement body with a vertical slope. This breakdown due to separation has been avoided in several conventional boundary-layer approaches by making various assumptions about the separated region such as that presented in reference 1 for supercritical airfoils and reference 2 for axisymmetric boattail flows. This singularity can be eliminated by solving the boundary-layer equations inversely; that is, the displacement thickness is prescribed and the pressure distribution is deduced from the boundary-layer solution. In reference 3, a recently-developed inverse boundary-layer formulation and finite-difference solution technique is presented and its applicability to turbulent separated flows is demonstrated. This new boundary-layer procedure can be used in either the direct mode (pressure prescribed, attached flow) or inverse mode (displacement thickness prescribed), and is no more complicated than conventional solution techniques.

The present difficulty in using an inverse boundary-layer technique is the coupling of such a procedure to a simultaneous computation of the inviscid flow to iteratively solve for the viscous-inviscid interaction. Some progress has been made in this area with the development of the interaction procedures given in references 4 and 5 for low-speed laminar flows and references 6 and 7 for transonic turbulent flows. However, significant improvements are needed in the first three of these techniques since they have various limitations and have not received widespread use. The technique developed by Thiede in reference 7 appears to be quite promising as it combines an inverse integral boundary-layer technique with a relaxation solution of the exact potential equation through a novel matching procedure presented in reference 8. Unfortunately, Thiede only presented the outline of this interaction procedure; further details are required in order to implement this scheme.

The purpose of this report is to present a new interaction procedure which permits the inverse boundary-layer procedure reported recently in reference 3 to be combined with an existing inviscid flow analysis. This new interaction technique is demonstrated by presenting solutions for the separated turbulent flow over axisymmetric body sting juncture which is schematically shown in figure 1. The inviscid calculations were made with an axisymmetric transonic code called RAXBOD. This code, which numerically solves the exact potential equation by relaxation, was originally developed by South and Jameson (ref. 9) and later modified and documented in reference 10. These calculations are for low-speed flow only; however, work is underway to extend these calculations to transonic speeds using the compressible inverse boundary-layer procedure in reference 3. This new interaction procedure, which is simple and converges rapidly, should be equally applicable to two-dimensional flows such as that over an airfoil, provided an appropriate inviscid code is used.

SYMBOLS

C_f	skin friction coefficient
C_p	coefficient of pressure
H	boundary-layer shape factor
i	interaction iteration index
Re_∞	Reynolds number based on free stream velocity and body length
r_o	body radius
u	velocity component parallel to body surface
u_e	velocity component parallel to body surface at edge of boundary layer
u_{e_V}	u_e predicted by viscous calculation
u_{e_I}	u_e predicted by inviscid calculation
v_n	normal velocity component at body surface
x	coordinate measured along body surface
δ^*	displacement thickness
θ	momentum thickness
ω	relaxation parameter

ρ density

τ_ω shear stress at body surface

VISCOUS ANALYSIS

The inverse boundary-layer technique used in the present calculations is the δ^*-prescribed procedure presented in reference 3, which is a finite-difference technique for the two-dimensional incompressible boundary-layer equations. For the present application, the Mangler transformation (ref. 11) is used to convert the two-dimensional boundary-layer solution to the required axisymmetric solution. In the present investigation, the Crank-Nicolson finite-difference scheme used in reference 3 was replaced with a first-order accurate scheme to suppress the streamwise oscillations which occurred in the body-sting juncture region. The first-order accurate scheme has greater streamwise damping than the second-order accurate Crank-Nicolson scheme, which has neutral stability in the wall region. This same modification was used in a previous investigation reported in reference 12 in which oscillations resulted when the Crank-Nicolson scheme was used to solve the boundary-layer equations subject to discontinuous wall suction.

In the present calculations, even with the first-order scheme, some oscillations still occurred in the solution unless the term $\frac{\partial u\delta^*}{\partial x}$, which appears in the x-momentum equation, was differenced in its conservative (unexpanded) form. With m used to denote the x-grid point index, the conservative differencing of this term gives

$$\left.\frac{\partial u\delta^*}{\partial x}\right|_m = \frac{(u\delta^*)_m - (u\delta^*)_{m-1}}{\Delta x} + O(\Delta x) \qquad (1)$$

where $O(\Delta x)$ is the first-order truncation error. In the previous study (ref. 3) this issue did not arise since both the conservative and nonconservative form of this term results in the same finite-difference expression, which is given as follows, when the Crank-Nicolson scheme is used:

$$\left.\frac{\partial u\delta^*}{\partial x}\right|_{m-\frac{1}{2}} = \frac{(u\delta^*)_m - (u\delta^*)_{m-1}}{\Delta x} + O(\Delta x^2) \tag{2}$$

INVISCID ANALYSIS

The inviscid calculations were done with a program called RAXBOD (ref. 10) which solves the finite-difference form of the exact potential equation by successive line overrelaxation for the transonic (or subsonic) inviscid flow over axisymmetric bodies in free air. For bodies with a sting this program uses a body-normal coordinate on the forebody up to the first horizontal tangent and a sheared cylindrical coordinate system aft of that point. This coordinate system seems particularly well suited to bodies which have sharp corners as demonstrated by South and Jameson (ref. 9). A stretching is applied to both the normal and tangential coordinates such that the infinite physical space is mapped to a finite computational space. A typical mesh distribution is shown in figure 2. This program is easy to use and has been combined by several investigators such as Wilmoth (ref. 2) with direct (pressure prescribed) boundary-layer calculations.

INTERACTION PROCEDURE

The iterative procedure, which is shown in figure 3, begins with an initial guess for δ^*, the displacement thickness distribution, which is then input to the inverse boundary-layer code; and the resulting solution yields the viscous edge velocity. The displacement effect of the viscous layer on the external inviscid flow is represented by prescribing, in the inviscid flow computation, an injection (or suction) velocity at the body surface which is given by

$$v_n = \frac{1}{r_o}\frac{d}{dx}(\delta^* u_e r_o) \tag{3}$$

for axisymmetric incompressible flow. This representation of the boundary layer is equivalent, but preferable, to adding the displacement thickness to the original body; in the latter case a recomputation of the inviscid mesh and a complete restart of the inviscid solution is required for each interaction cycle. Use of equation (3) affects only the surface boundary condition in the inviscid calculation and thus does not require significant modifications be made to the inviscid code. The output from the inviscid calculation which is made with RAXBOD in the present case, is the inviscid surface tangential velocity.

The next step in the interaction procedure is the computation of the new displacement thickness distribution which, as shown in figure 3, is deduced from the mismatch of the viscous and inviscid tangential velocities by

$$\delta^*_{new} = \delta^*_{old}\frac{u_{e_V}}{u_{e_I}} \tag{4}$$

This update procedure for the displacement thickness is the key link which allows an inverse boundary-layer computation to be combined with a direct inviscid flow analysis. The iterative process continues until convergence is obtained when the new and old displacement thickness distributions differ by less than a specified tolerance.

This new update procedure for the displacement thickness was originally an ad hoc assumption, but further examination shows that it is somewhat analogous to the relationship between changes in u_e and δ^* given by the von Karman momentum integral

$$\frac{d\theta}{dx} + \frac{2\theta + \delta^*}{u_e}\frac{du_e}{dx} = \frac{\tau_\omega}{\rho u_e^2} \tag{5}$$

If the shape factor $H \equiv \frac{\delta^*}{\theta}$ is introduced and its streamwise variation is neglected, then equation (5) can be approximately written as

$$d\delta^* \approx -(H + 2)\frac{\delta^*}{u_e}du_e + Hdx\frac{\tau_\omega}{\rho u_e^2} \tag{6}$$

The update procedure on the displacement thickness, including a relaxation parameter ω, can be written as

$$\delta^{*i+1} = \delta^{*i} + \omega\delta^{*i}\left(\frac{u_{e_V}}{u_{e_I}} - 1\right) \tag{7}$$

where if $\omega = 1$ equation (4) is obtained. With the definition

$$\Delta u_e = u_{e_I} - u_{e_V} \tag{8}$$

and correspondingly

$$\Delta\delta^* = \delta^{*i+1} - \delta^{*i} \tag{9}$$

Equation (7) can be rearranged to give the approximate relation

$$\Delta\delta^* \approx -\omega\frac{\delta^*}{u_e}\Delta u_e \tag{10}$$

Comparison of equations (6) and (10) shows that they are quite similar in rela g an increment in u_e to that in δ^*, particularly where the skin friction is small. It is recognized that this comparison is not exact since the increments in u_e and δ^* in the momentum integral equation are changes in the streamwise direction whereas those in equation (10) refer to changes between successive interaction cycles. Nonetheless, there seems to be some merit to this comparison since; for example, an alternate δ^* update procedure given by

$$\delta^{*i+1} = \delta^{*i} + \omega\left(\frac{u_{e_I}}{u_{e_v}} - 1\right) \tag{11}$$

which is not analogous to the momentum integral equation was found to be divergent. Following the same steps which led to equation (10), equation (11) can be approximately written as

$$\Delta\delta^* \approx \omega \frac{\delta^*}{u_e} \Delta u_e \tag{12}$$

which differs in sign from equation (10).

Most viscous-inviscid interaction schemes require underrelaxation ($\omega < 1$) for convergence, but in the present calculations it was found that overrelaxation ($\omega > 1$) could be used to accelerate the convergence of the interaction process. The similarity between equations (6) and (10) offers an explanation since, even with overrelaxation, it was observed in the present calculations that

$$\omega < H + 2 \tag{13}$$

since H typically varies from 1 to 2.5, while ω had to be restricted to values less than 2 to avoid divergence.

RESULTS AND DISCUSSION

Interaction results obtained with this procedure were obtained for the turbulent incompressible flow over ellipsoids with 10/1 and 10/3 axis ratios and stings which are 20 percent and 33 percent, respectively, of the maximum body radius. A small fillet was inserted between the body and sting to avoid a slope discontinuity. The initial δ^* distribution that was used to initialize the interaction procedure was obtained from a direct boundary-layer computation using a modified inviscid tangential surface velocity as shown in figure 4 for the 10/3 ellipsoid. This boundary-layer computation was made with the same program that was used in the inverse calculations since, as discussed in reference 3, either the direct or inverse option can be exercised in this boundary-layer formulation with only a simple boundary condition change required. It was necessary to flatten the inviscid velocity distribution such that the boundary layer did not separate and give a singularity in the initial direct boundary-layer computation. Figure 4 also shows, for comparison, the final interacted tangential velocity distribution.

The present calculations are intended only to demonstrate this new interaction procedure and thus, to simplify the calculations, the interaction was assumed to be negligible upstream of the maximum body radius. At this point, the turbulent boundary-layer profile was assumed to be given by Coles' (ref. 13) wall-wake formulation with the edge velocity given by the uninteracted inviscid computation. Values for the boundary-layer thickness and skin-friction coefficient, which are also required in the wall-wake formulation, were assumed and are typical of a turbulent boundary layer at a local Reynolds number of 7.5×10^5 in a zero pressure gradient.

In the present calculations, 93 grid points were used across the boundary layer and 80 in the streamwise direction. The inviscid calculation was made with 81 and 41 grid points in the streamwise and lateral directions, respectively. The downstream boundary in the inviscid computation was placed at approximately the same location as that used in the boundary-layer computation. The velocity potential along this boundary was obtained by quadratic extrapolation of the upstream values. No problems were encountered using this procedure since the boundary was placed sufficiently far downstream where the flow velocity had nearly recovered to the free-stream value.

The interacted results for the pressure, displacement body, and skin friction are shown in figures 5 and 6 for the 10/1 and 10/3 ellipsoids, respectively. The Reynolds number used in these calculations is 1.53×10^6 based on the body length and free-stream velocity. Attached flow was computed for the 10/1 ellipsoid as shown in figure 5(b); separated flow, for the 10/3 ellipsoid, as shown in figure 6(b). The points of separation and reattachment are denoted as S and R, respectively, in figure 6. In both cases near the upstream boundary the interacted pressure differs only slightly from that obtained in the inviscid calculation and thus it is a reasonable assumption to neglect the boundary layer upstream of the maximum body radius. Figures 5(a) and 6(a) show typical interaction results, where it is seen that the inclusion of the boundary layer results in pressure distributions with smaller gradients than the corresponding inviscid distributions.

In these calculations a boundary-layer calculation was made after every 20 relaxation cycles in the inviscid code RAXBOD. Further study needs to be made to determine the optimum number of inviscid cycles between boundary-layer computations so as to reduce computer time. The 10/1 ellipsoid took about 7 interactions for convergence and required about 1.5 minutes of CDC

CYBER-175 computer time. The 10/3 ellipsoid took about 10 iterations and 2 minutes of computer time for convergence.

Conventional viscous-inviscid matching techniques generally require, even for mild interaction cases, numerical smoothing and underrelaxation after each interaction iteration to prevent divergence. In contrast, the present calculations, in which the interaction is quite significant, required no smoothing or underrelaxation. Smoothing is probably not needed in the present interaction procedure since it naturally occurs in the inverse boundary-layer calculation when the tangential velocity, u_e, is computed by integrating the pressure gradient deduced in the calculation. Numerical integration tends to smooth the results in contrast to numerical differentiation, which occurs in direct boundary-layer techniques where the imposed pressure gradient is computed by numerically differentiating the inviscid pressure distribution.

The convergence of the interaction calculation was accelerated somewhat as shown in figure 7 by using overrelaxation, $\omega = 1.5$. In figure 7(a), six streamwise locations along the displacement thickness distribution are indicated. In figures 7(b) and 7(c) the convergence history of the displacement thickness at these six locations is shown for both $\omega = 1$ and $\omega = 1.5$. It is seen that the use of overrelaxation has the greatest effect in reducing the number of iteration cycles at locations c and d, where the interaction is the strongest. Overrelaxation was used for only five interaction cycles as it was found that an oscillatory pattern in the convergence history persisted if overrelaxation was used throughout. Although the effect shown here of overrelaxation is relatively small, it does appear that the present interaction procedure is very promising. Further study is needed to deduce an optimum value of the overrelaxation parameter.

CONCLUDING REMARKS

Converged solutions obtained with this new interaction procedure demonstrate that this technique may be quite useful for flows with strong interaction including small separated regions. The present approach may even be preferable to existing interaction schemes for attached flow since the present procedure, in the calculations reported, required no smoothing and over-relaxation was used. This procedure should now be extended to compressible flow and comparisons made with experimental data. Since the present boundary-layer approach is a finite-difference technique, the present interaction procedure should be quite useful for testing various turbulence models to improve the current capability in predicting the detailed characteristics of separated turbulent flow.

REFERENCES

1. Bauer, Frances; Garabedian, Paul; Korn, David; and Jameson, Antony: Supercritical Wing Sections, II. Springer-Verlag Publisher, 1975.
2. Wilmoth, Richard G.: Computation of Transonic Boattail Flow With Separation. NASA TP 1070, 1977.
3. Carter, James E.: Inverse Boundary-Layer Theory and Comparison With Experiment. NASA TP 1208, 1978.
4. Carter, James E.; and Wornom, Stephen F.: Solutions for Incompressible Separated Boundary Layers Including Viscous-Inviscid Interaction. Aerodynamic Analyses Requiring Advanced Computers, Part I, NASA SP-347, 1975, pp. 125-150.
5. Davis, R. T.; and Werle, M. J.: Numerical Methods for Interacting Boundary Layers. Univ. of Cincinnati Rept. No. AFL 76-8-23, Aug. 1976.
6. Kuhn, Gary D.; and Nielsen, Jack N.: Prediction of Turbulent Separated Boundary Layers. AIAA Paper No. 73-663, July 1973.
7. Thiede, P. G.: Prediction Method for Steady Aerodynamic Loading on Airfoils With Separated Transonic Flow. AGARD CP-204, Prediction of Aerodynamic Loading, Sept. 27-29, 1976.
8. Brune, G. W.; Rubbert, P. E.; and Nark, T. C., Jr.: New Approach to Inviscid Flow/Boundary-Layer Matching. AIAA J., vol. 13, no. 7, pp. 936-938, July 1975.
9. South, Jerry C., Jr.; and Jameson, Antony: Relaxation Solutions for Inviscid Axisymmetric Transonic Flow Over Blunt or Pointed Bodies. AIAA Computational Fluid Dynamics Conference, Palm Springs, Calif., pp. 8-17, July 1973.
10. Keller, James D.; and South, Jerry C., Jr.: RAXBOD: A Fortran Program for Inviscid Transonic-Flow Over Axisymmetric Bodies. NASA TM X-72831, Feb. 1976.
11. Schlichting, Hermann (Kestin, J., transl.): Boundary Layer Theory. Fourth ed., McGraw-Hill Book Co., Inc., c. 1960.
12. Carter, James E.: STAYLAM: A Fortran Program for the Suction Transition Analysis of a Yawed Wing Laminar Boundary Layer. NASA TM X-74013, March 1977.
13. Coles, D.: The Law of Wake in the Turbulent Boundary Layer. J. Fld. Mech., vol. 1, pp. 191-225, 1956.

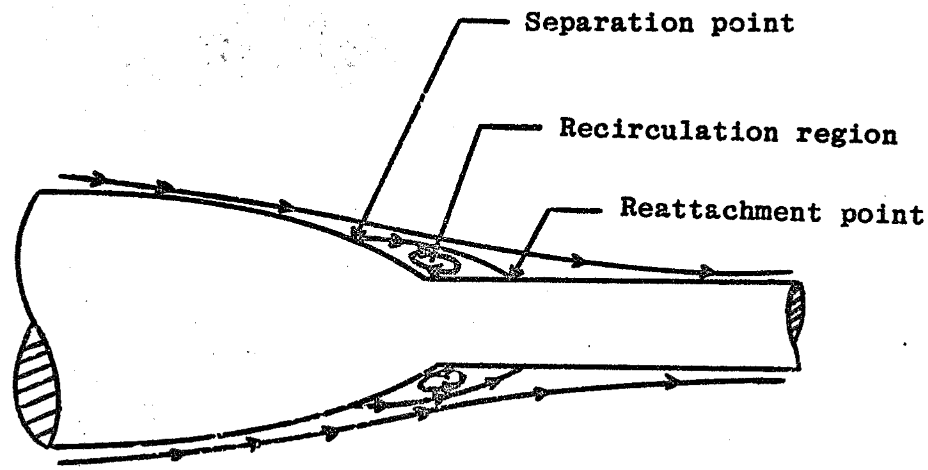

Figure 1.- Schematic diagram of separated flow at axisymmetric body-sting juncture.

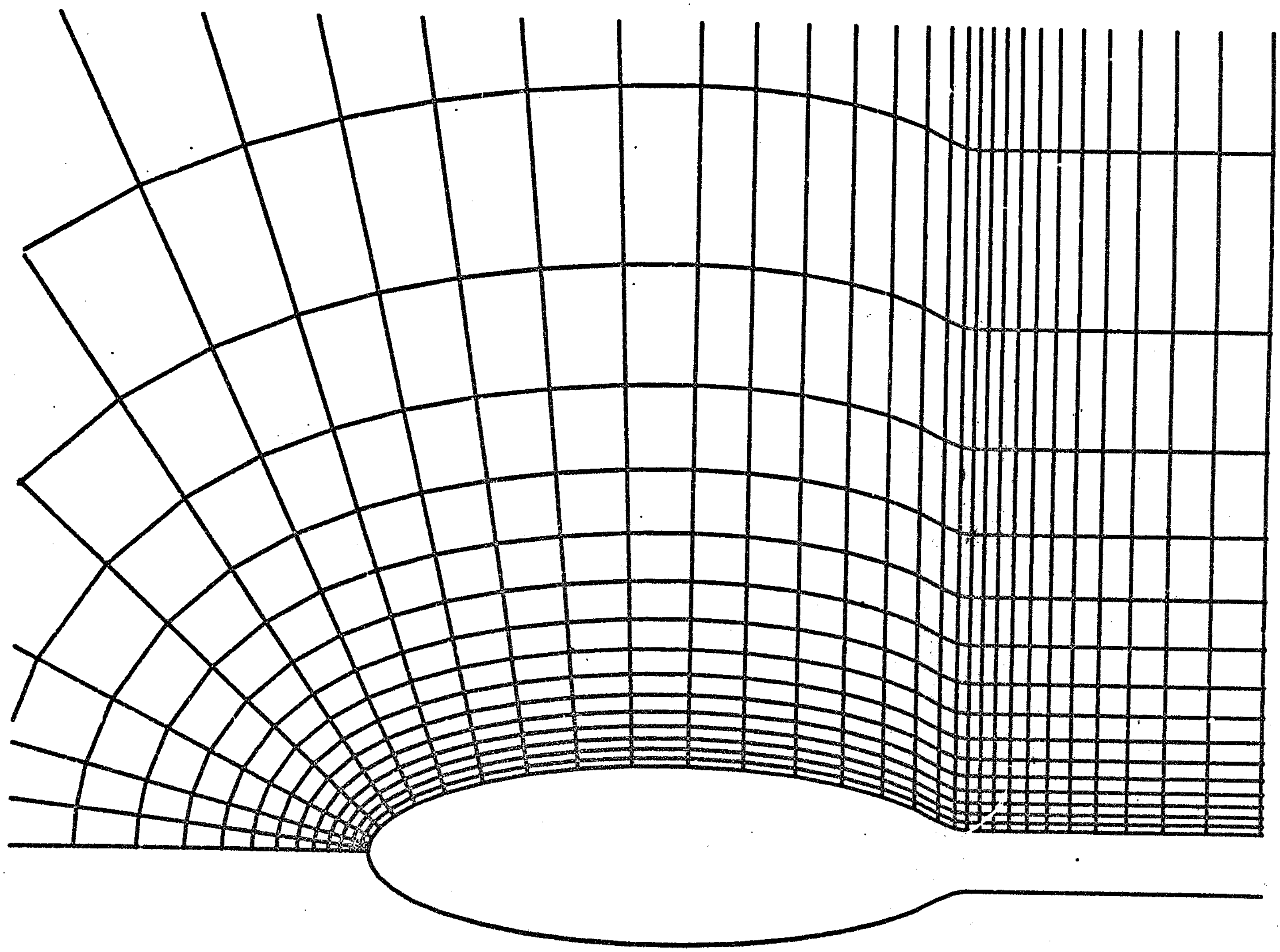

Figure 2.- Inviscid computational mesh.

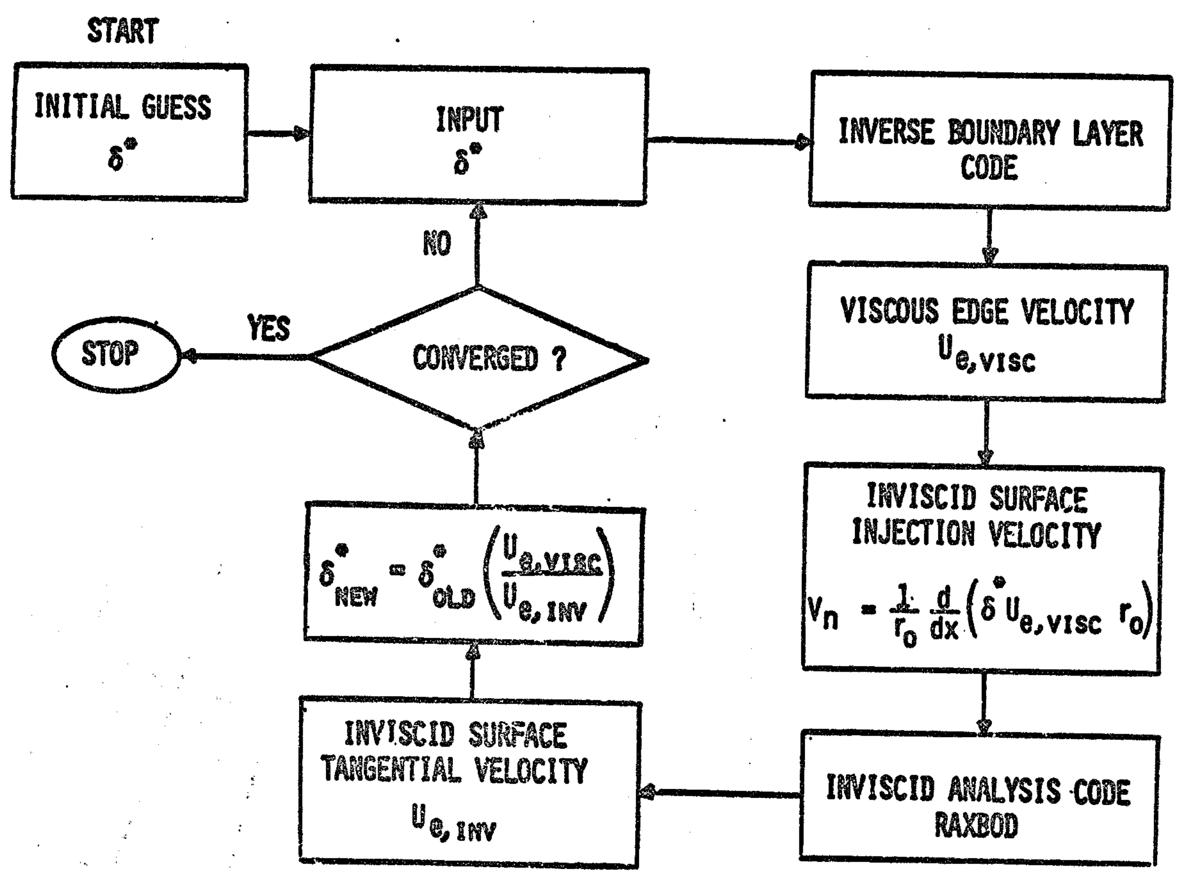

Figure 3.- Inverse boundary layer/inviscid interaction.

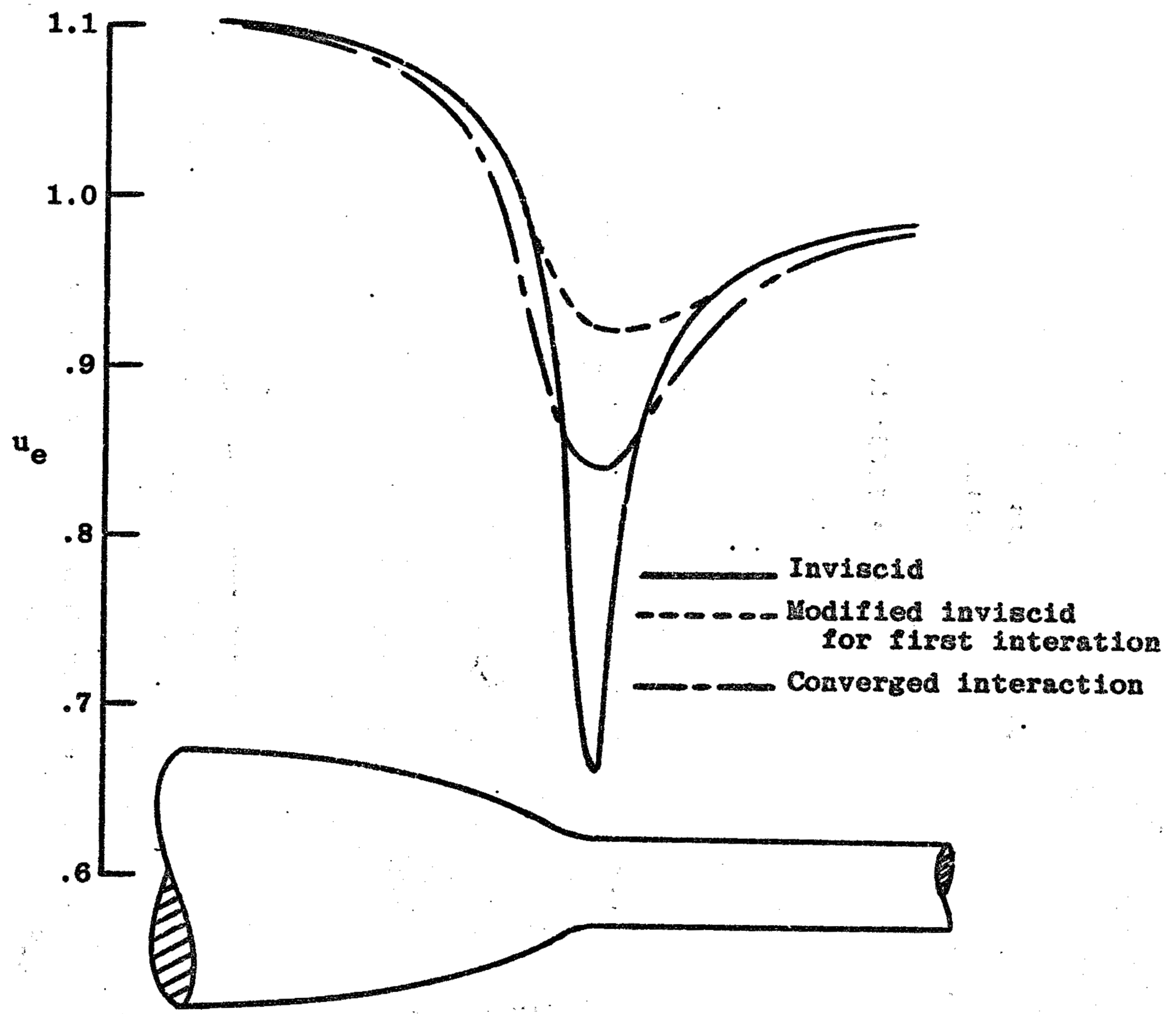

Figure 4.- Inviscid, initial and interacted tangential velocity distributions.

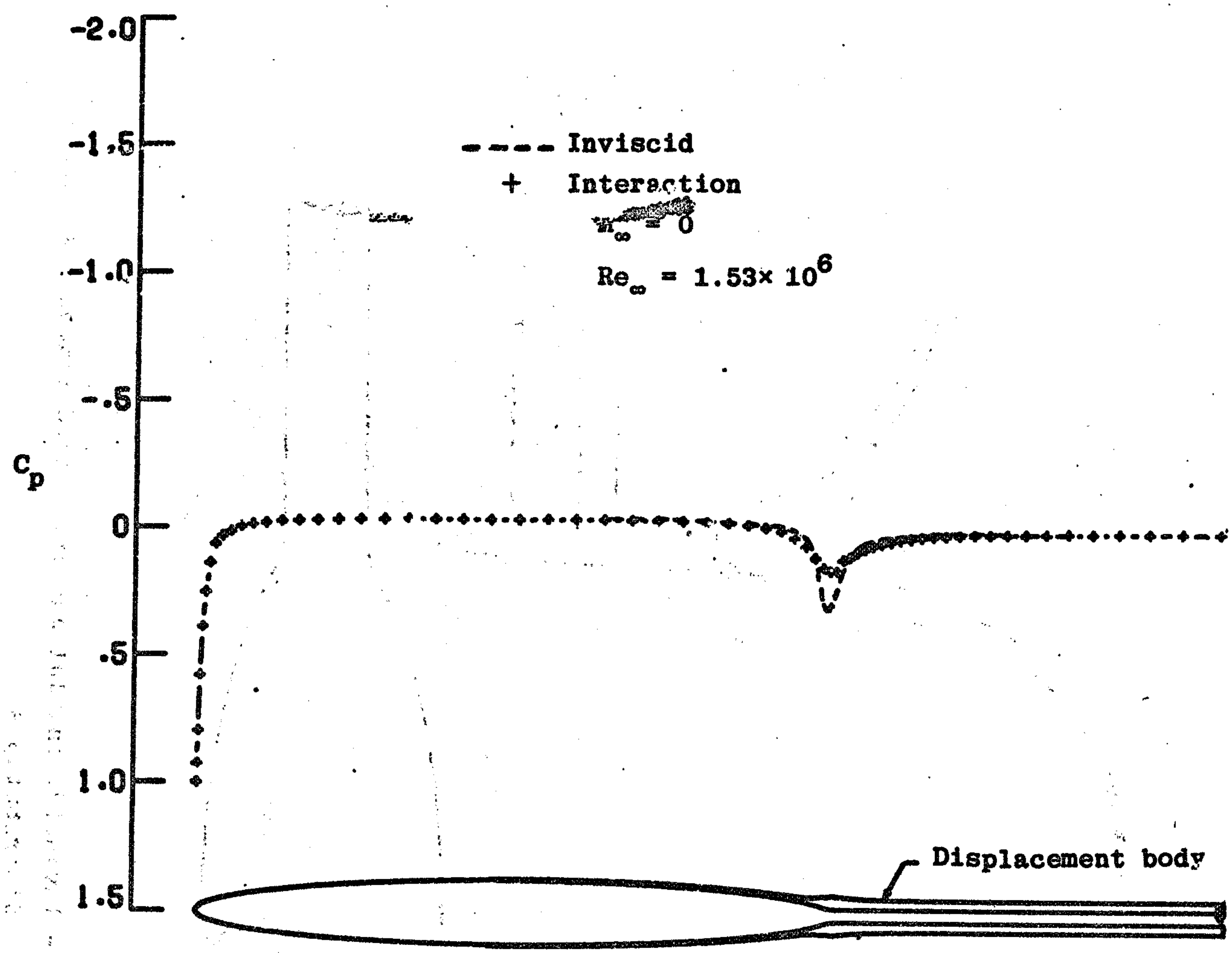

(a) Pressure distribution and displacement body.

Figure 5.- Interaction results for 10/1 ellipsoid w/20% sting.

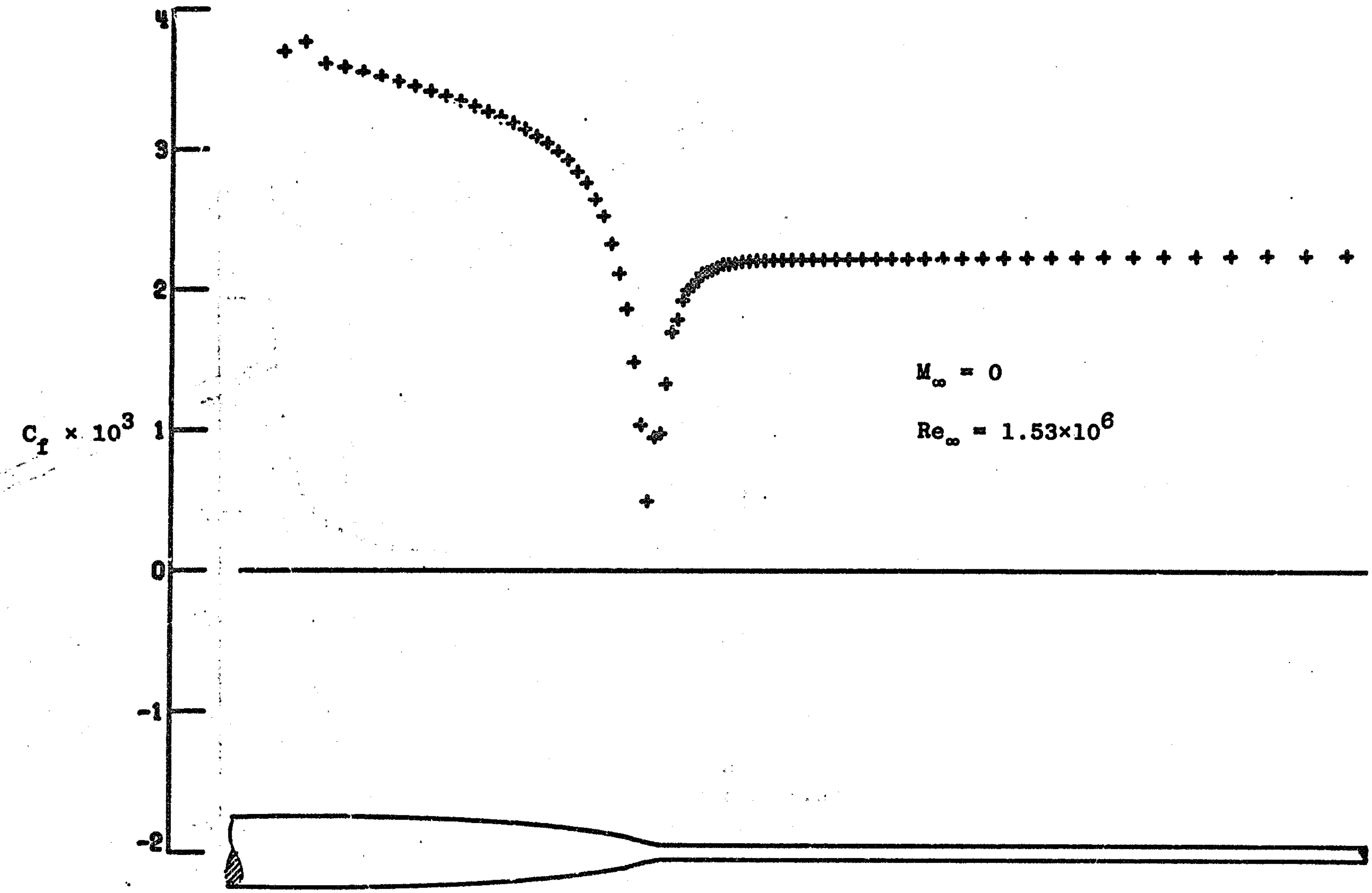

(b) Skin friction distribution.

Figure 5.- Concluded.

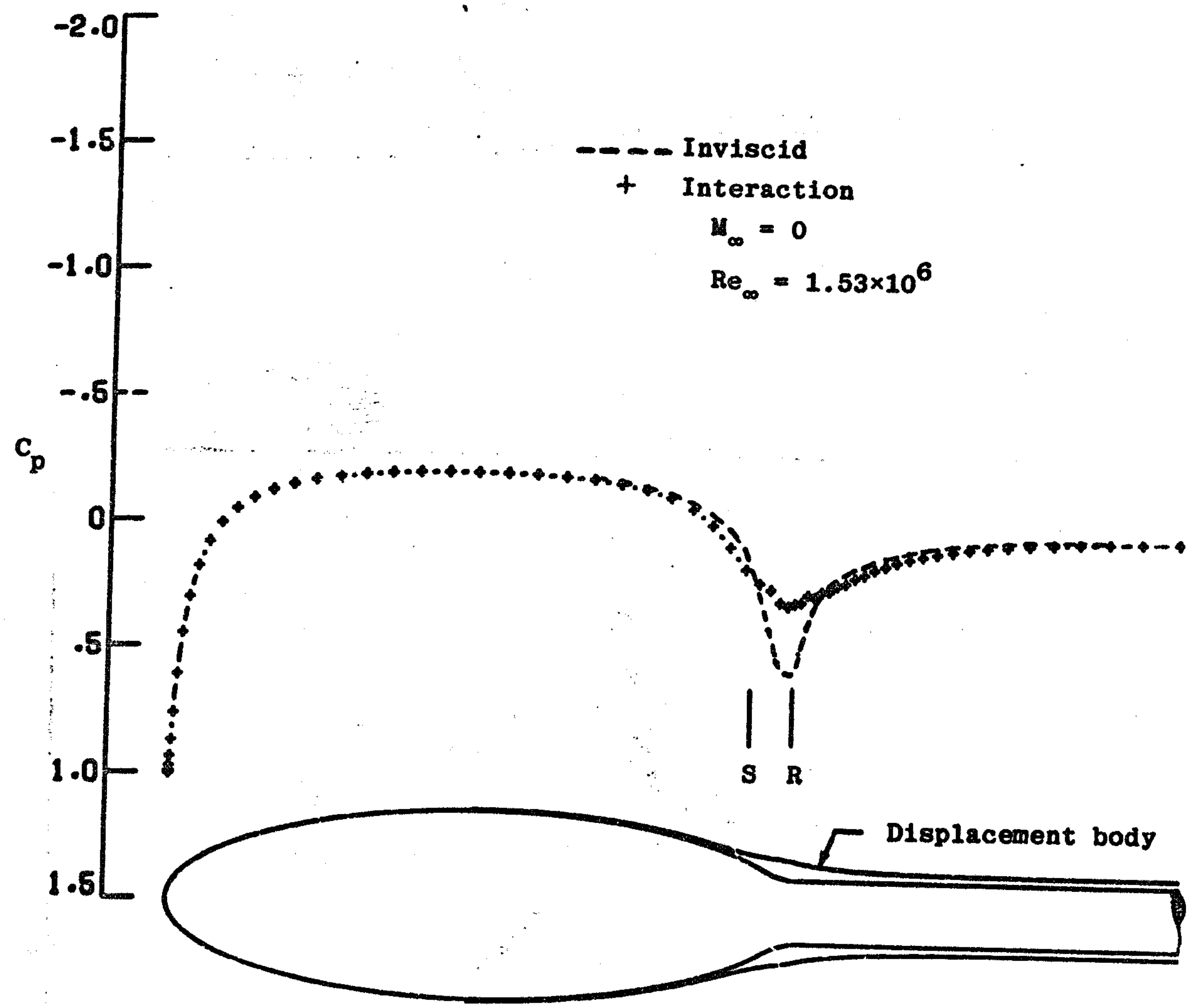

(a) Pressure distribution and displacement body.

Figure 6.- Interaction results for 10/3 ellipsoid with 33 % sting.

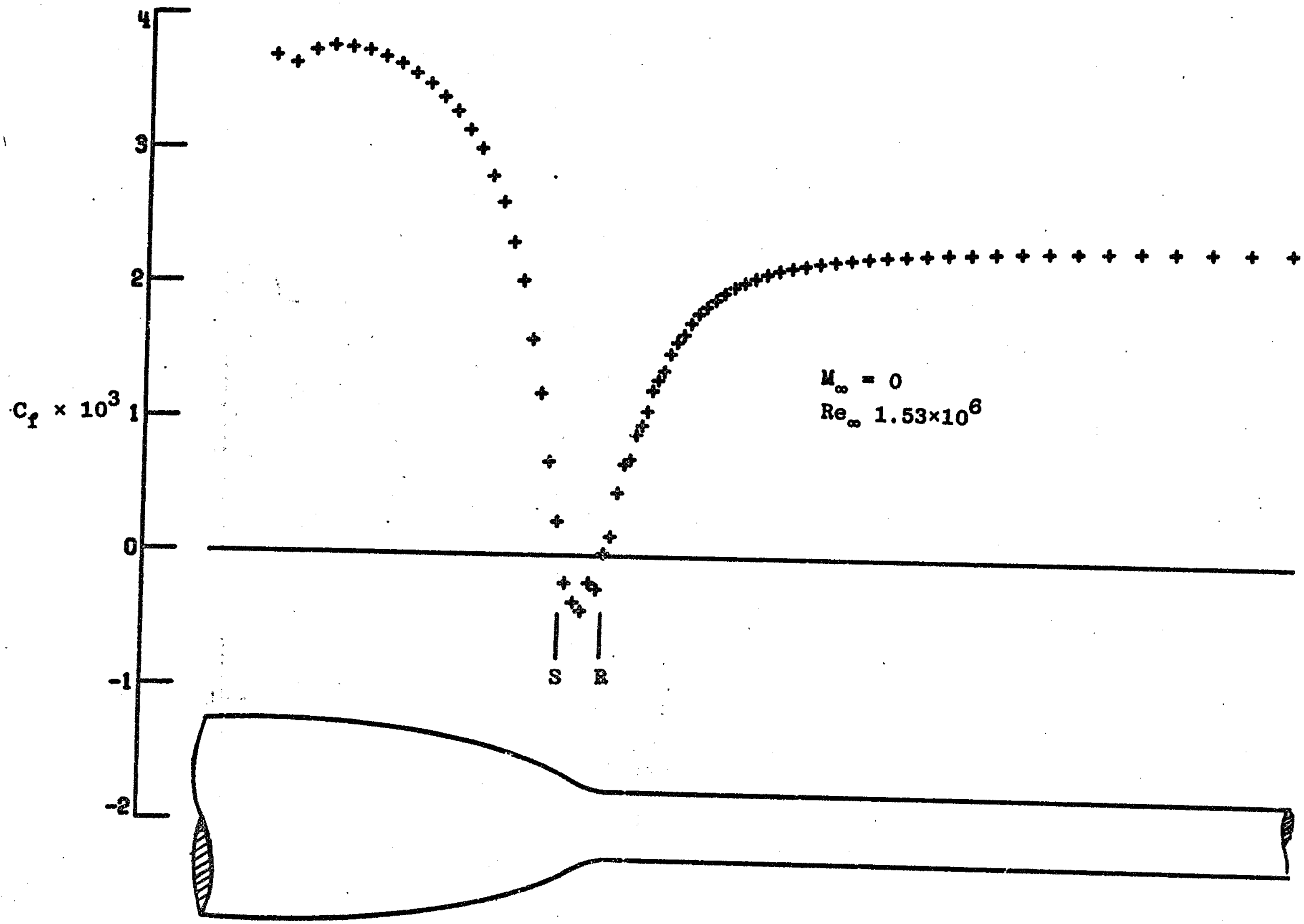

(b) Skin friction distribution.

Figure 6.- Concluded.

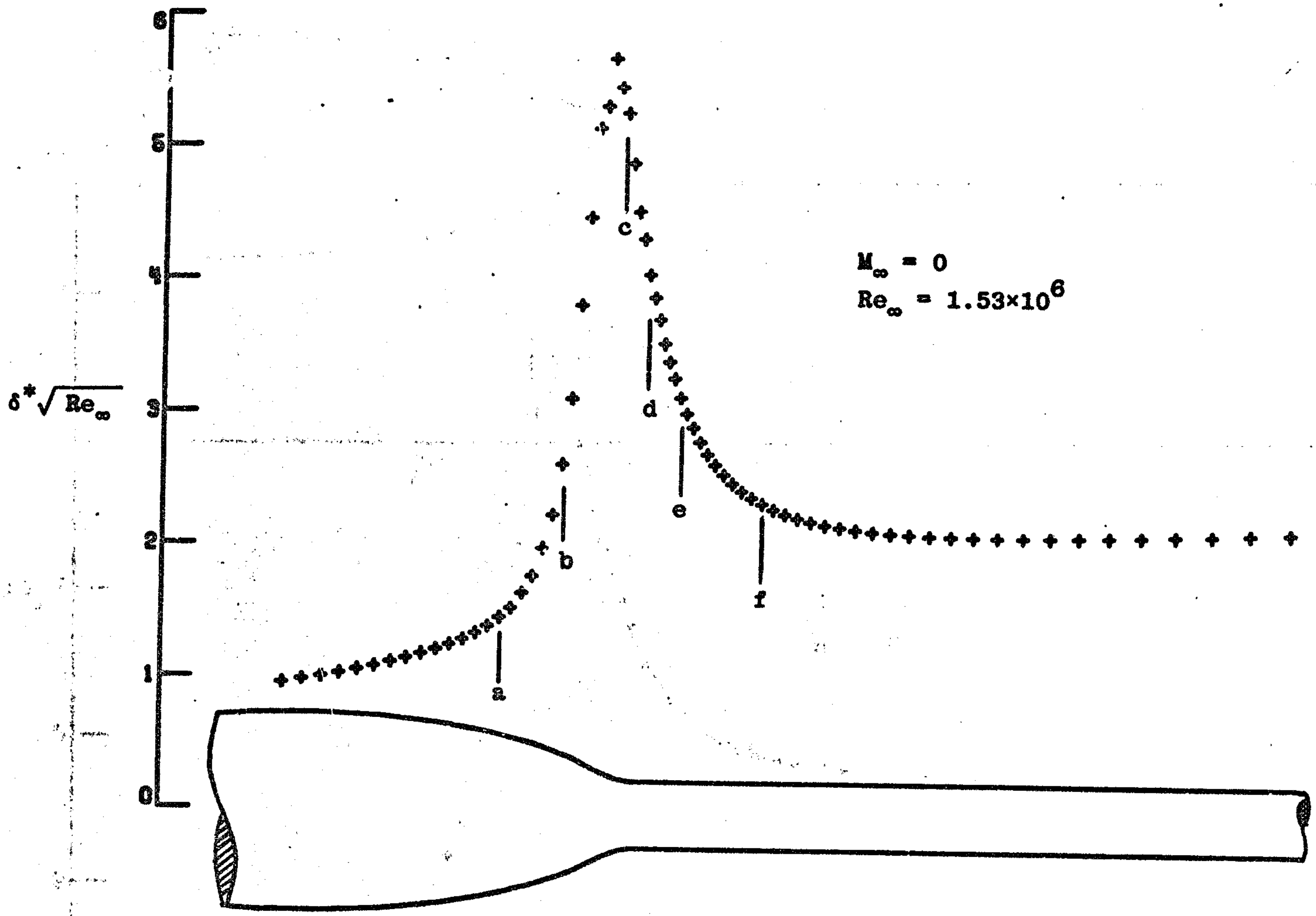

(a) Displacement thickness distribution and locations where interaction convergence is plotted.

Figure 7.- Acceleration of interaction convergence by overrelaxation.

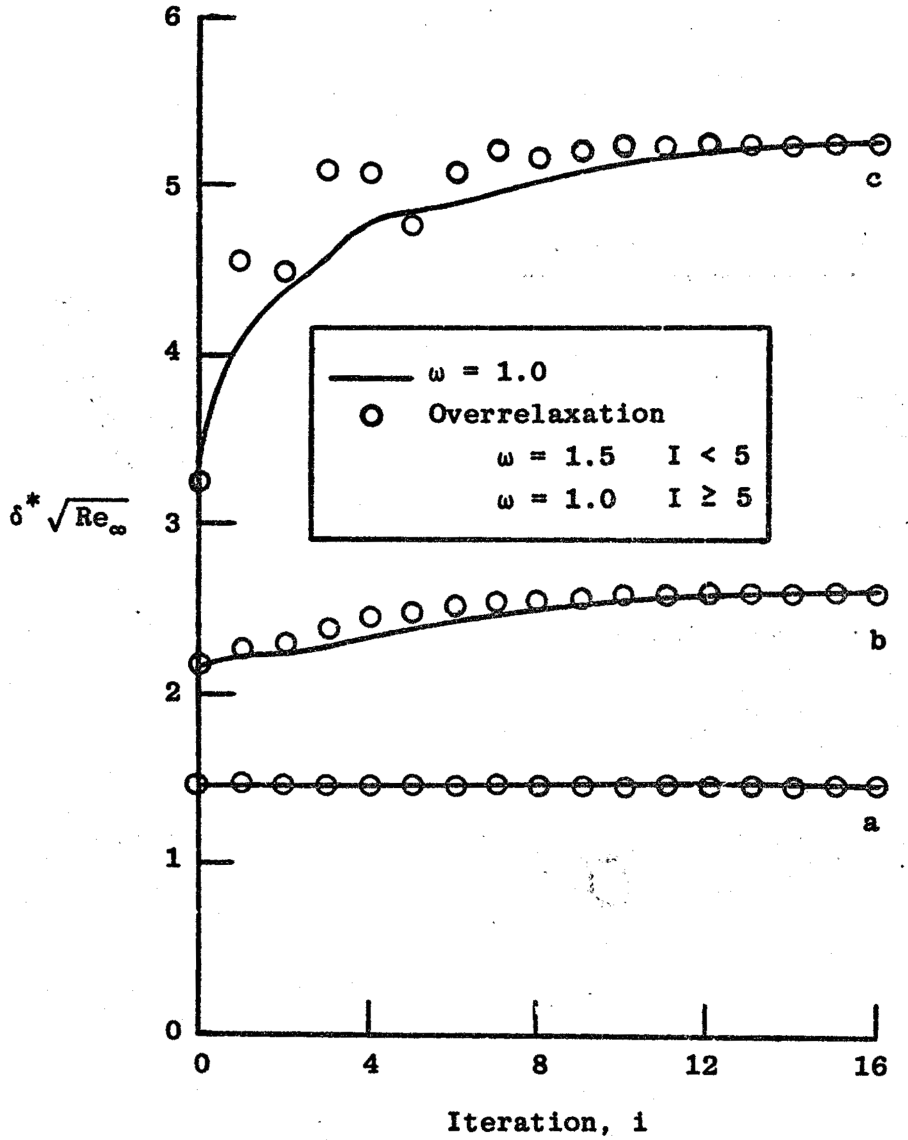

(b) Displacement thickness convergence at locations a, b, and c.

Figure 7.- Continued.

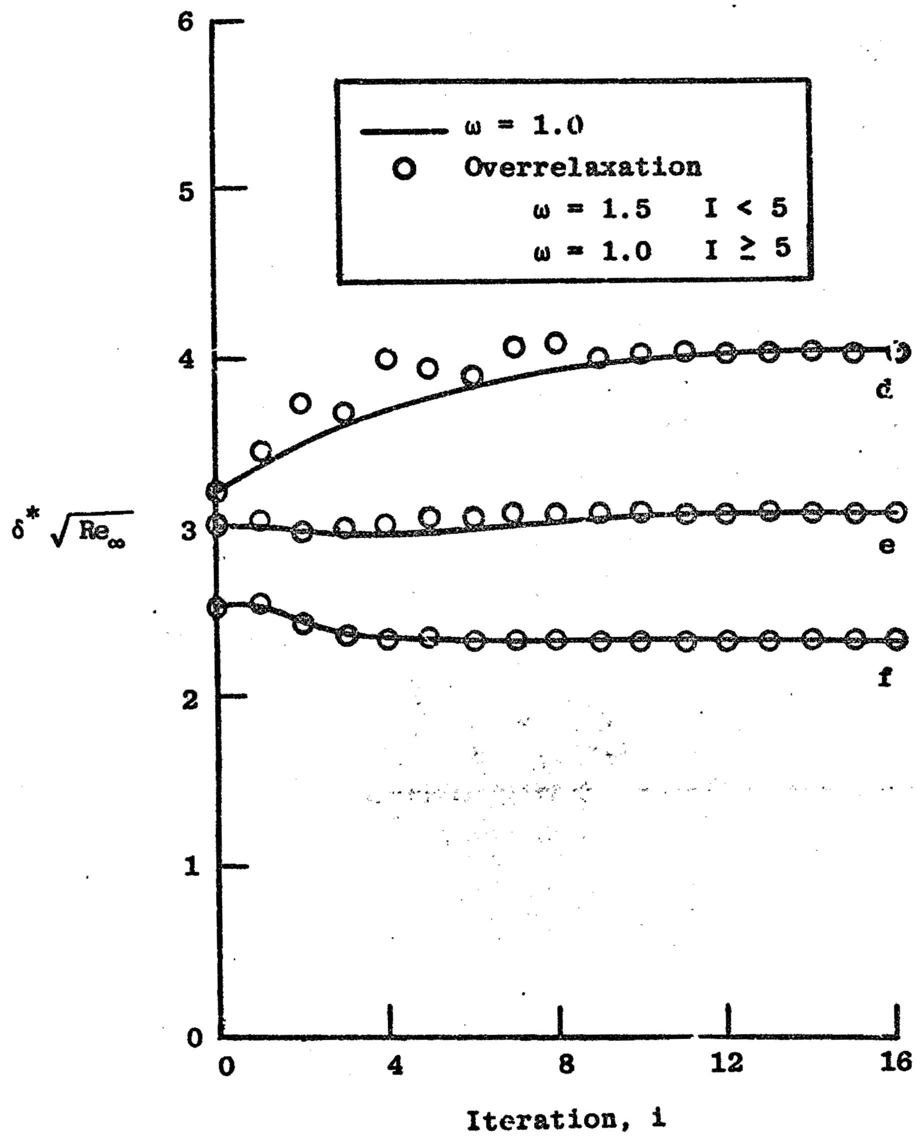

(c) Displacement thickness convergence at locations d, e, f.

Figure 7.- Concluded.